

Ordered Mesoporous Carbon and Thiolated Polyaniline Modified Electrode for Simultaneous Determination of Cadmium(II) and Lead(II) by Anodic Stripping Voltammetry

Lin Tang,^{*,[a, b]} Jun Chen,^[a, b] Guangming Zeng,^{*,[a, b]} Yuan Zhu,^[a, b] Yi Zhang,^[a, b] Yaoyu Zhou,^[a, b] Xia Xie,^[a, b] Guide Yang,^[a, b] and Sheng Zhang^[a, b]

Abstract: The fabrication and evaluation of a glassy carbon electrode (GCE) modified with ordered mesoporous carbon (OMC), 2-mercaptoethanesulfonate (MES)-tethered polyaniline (PANI) and bismuth for simultaneous determination of trace Cd^{2+} and Pb^{2+} by differential pulse anodic stripping voltammetry (DPASV) are presented here. The morphology and electrochemical properties of the fabricated electrode were respectively characterized by scanning electron microscopy (SEM) and electrochemical impedance spectroscopy (EIS). Experimental parameters such as PANI disposition, preconcentration

potential, preconcentration time and bismuth concentration were optimized. Under optimum conditions, the fabricated electrode exhibited linear calibration curves ranged from 1 to 120 nM for Cd^{2+} and Pb^{2+} . The limits of detection (LOD) were 0.26 nM for Cd^{2+} and 0.16 nM for Pb^{2+} ($S/N=3$), respectively. Additionally, repeatability, reproducibility, interference and application were also investigated, and the proposed electrode exhibited excellent performance. The proposed method could be extended for the development of other new sensors for heavy metal determination.

Keywords: Ordered mesoporous carbon • Thiolated polyaniline • Stripping voltammetry • Cadmium • Lead

1 Introduction


Cadmium and lead are highly toxic heavy metals which have linked to various adverse effects on human health and ecosystem. The World Health Organization (WHO) recommends threshold limit values (TLV) of 3 $\mu\text{g/L}$ and 10 $\mu\text{g/L}$ for Cd^{2+} and Pb^{2+} in drinking water, respectively [1,2]. Several analytical techniques, including flame atomic absorption spectrometry (F-AAS), atomic emission spectrometry (AES) and inductively coupled plasma-mass spectrometry (ICP-MS) [3] have been used in the determination of trace heavy metals. However, the wide utilization of these techniques is limited due to the expensive instrumentation cost, time-consuming and labor intensive process, and the difficulty to be deployed on site [4,5]. On the other hand, electrochemical stripping analysis has been widely recognized as a powerful tool for measuring trace heavy metals because of its low cost, remarkable sensitivity, reliability and simplicity of measurement [6–10]. Recently, the bismuth-based chemically modified electrodes (CMEs) have been widely studied for the determination of Cd^{2+} and Pb^{2+} in association with anodic stripping voltammetry (ASV) in place of mercury-based electrodes, owing to its environment friendly property, low toxicity, wide potential window, and easy alloy formation ability with heavy metal ions [11–14].

Ordered mesoporous carbon (OMC) has attracted considerable attention as a chemically modifying material due to its extremely ordered and uniform pore structure,

high specific surface area, fast electron transfer rate and excellent electrocatalytic activity [15]. OMC based CMEs have been used in electrochemical analysis of many organic and inorganic analytes, e.g., phenols [16], glucose [17], morphine [18] and heavy metals [19]. In addition, conducting polymers (CPs), such as polyaniline (PANI), polypyrrole and polyacetylene, have superior electrical conductivities, good electrochromic property, redox reversibility and suitable structural characteristics [20,21], which aroused more interest among researchers. Electrochemical analysis of trace heavy metals using the conducting polymer modified electrodes has attracted increasing attention because of the enrichment of target heavy metals and improvement of analytical performance [22]. Interestingly, these conducting polymers in oxidized states of alkenes-like electron-conjugate structure can in-

[a] L. Tang, J. Chen, G. Zeng, Y. Zhu, Y. Zhang, Y. Zhou, X. Xie, G. Yang, S. Zhang
College of Environmental Science and Engineering, Hunan University Changsha, 410082, P. R. China
*e-mail: etanglin@126.com
zgming@hnu.edu.cn

[b] L. Tang, J. Chen, G. Zeng, Y. Zhu, Y. Zhang, Y. Zhou, X. Xie, G. Yang, S. Zhang
Key Laboratory of Environmental Biology and Pollution Control, Hunan University, Ministry of Education
Changsha 410082, P. R. China

 Supporting Information for this article is available on the WWW under <http://dx.doi.org/10.1002/elan.201400350>.

teract with thiols, which can be considered as a new researching branch of the thiol-ene chemistry [20,23,24]. The thiol-ene chemistry generally refers to the addition of an S-H bond across a double bond by either a free radical or ionic mechanism [25]. The introduction of thiol enhances CPs' stability, electroactivity and enrichment of heavy metals. Although CPs were widely used in electrochemical sensor, the thiolated CPs have been rarely used. Until recently, Chen et al. [20] have reported the synthesis of thiolated CPs for electrochemical analysis of heavy metals. The application of the thiolated CPs on heavy metal analysis is an attractive research.

The aim of this work is to combine the excellent characteristics of OMC and thiolated PANI to develop a sensitive CME for electrochemical analysis of trace Cd^{2+} and Pb^{2+} through differential pulse anodic stripping voltammetry (DPASV). OMC, PANI and 2-mercaptoethanesulfonate (MES) were modified on the glassy carbon electrode (GCE) surface in sequence to obtain a PANI-MES/OMC/GCE. Scanning electron microscopy (SEM) and electrochemical impedance spectroscopy (EIS) were used to study the morphology and properties of the above electrode. The performance of the electrode was evaluated in acetate buffer solution containing Cd^{2+} , Pb^{2+} , Bi^{3+} , and compared to the similar modified electrodes. Practical application has been examined in three different real samples.

2. Experimental

2.1 Apparatus

All electrochemical experiments were carried out with CHI 760D electrochemical workstation (Chenhua Instrument, Shanghai, China). Conventional three-electrode system was used in this work: a modified glassy carbon electrode (GCE, 3 mm diameter) as the working electrode, a KCl-saturated calomel electrode (SCE) as the reference electrode and a platinum wire as the counter electrode. Scanning Electron Microscopy (SEM) was carried out by S-4800 scanning electron microscope (Hitachi Ltd, Japan). Model PHSJ-3F laboratory pH meter (Leici Instrument, Shanghai, China) was used for pH measurements.

2.2 Reagents

OMC was synthesized in our lab according to the method reported by Ryoo and co-workers [26] with slight alterations [27]. SBA-15 as a silica template, sucrose was used as a carbon source. The OMC was synthesized by inserting carbon source into SBA-15, carbonizing at high temperature and removing silica template. Stock solutions of Cd^{2+} , Pb^{2+} and Bi^{3+} were prepared by dissolving $\text{Cd}(\text{NO}_3)_2$, $\text{Pb}(\text{NO}_3)_2$ and $\text{Bi}(\text{NO}_3)_3 \cdot 5\text{H}_2\text{O}$ into ultrapure water and stored at 4 °C. Acetate buffer solution (0.1 M, pH 4.5) was prepared by CH_3COOH and CH_3COONa and used as supporting electrolyte. Aniline was purchased

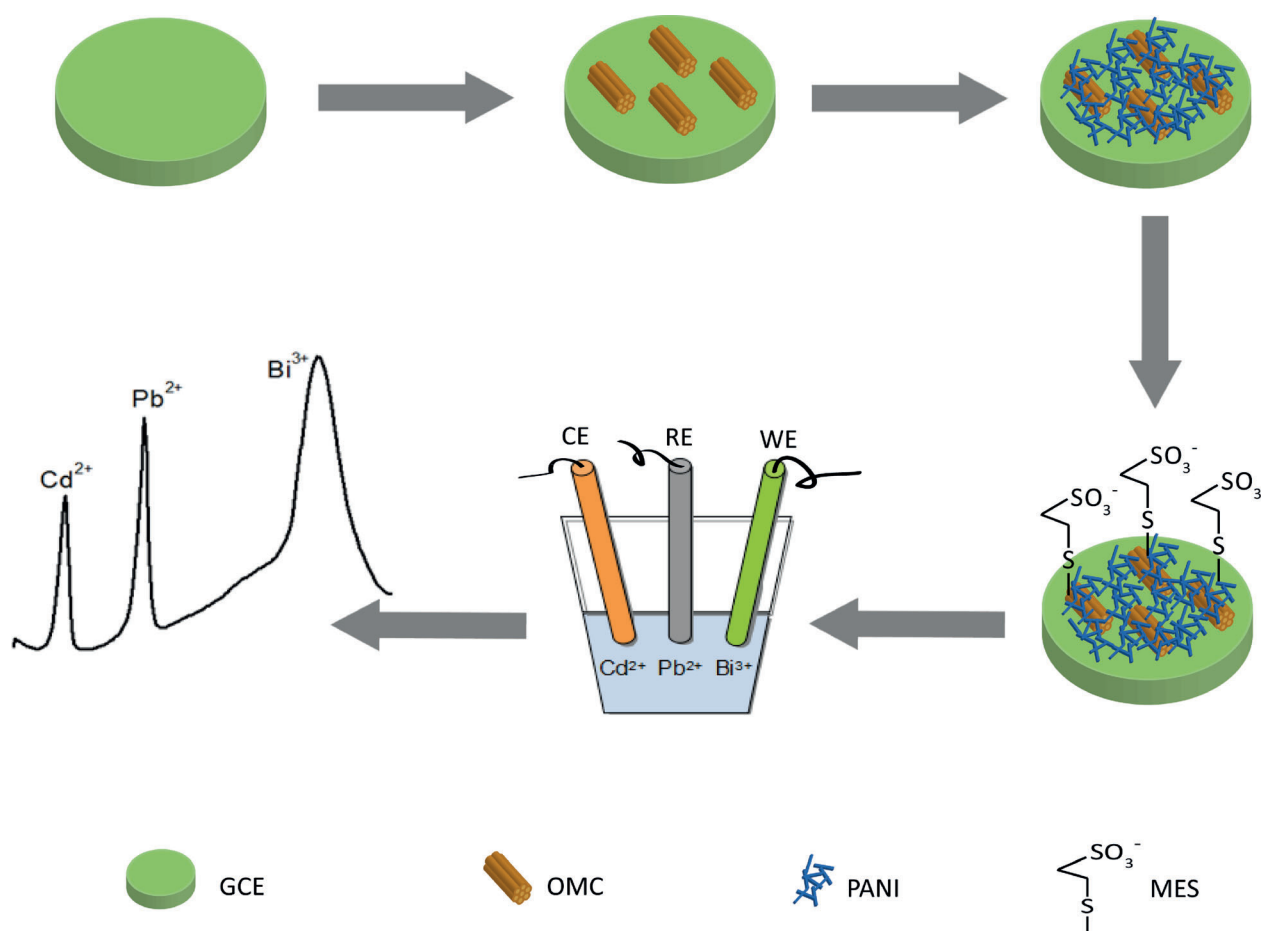
from the Sinopharm Chemical Reagent Co, Ltd (Shanghai, China) and purified twice under reduced pressure and then stored in refrigerator prior to use. MES was purchased from Aladdin (China). All chemicals were of analytical grade and used as received; all the solutions were prepared with ultrapure water.

2.3 Fabrication of the Working Electrode

The bare GCE was first polished sequentially with 1, 0.3 and 0.05 μm alumina powders on a soft cloth, and then sonicated in ethanol and ultrapure water for 3 min, respectively. Then, the GCE was scanned by cyclic voltammetry in 0.5 M H_2SO_4 between -0.4 V and 0.8 V (vs. SCE) at 100 mV/s to reach a steady state. Different solvents (*N,N*-dimethylformamide (DMF), pure water) were tried for OMC dispersion, and the mixture was sonicated for 1 h. The results showed that OMC can be dispersed with DMF to form a 0.5 mg/mL stable and homogeneous suspension. The fabrication of PANI-MES/OMC/GCE was carried out as follows. First, 5.0 μL OMC suspension was dripped onto GCE surface and dried in air to form an OMC/GCE. The resulted "OMC film" has good adhesion and will not peel off. Then, the OMC/GCE was scanned by cyclic voltammetry in the mixed solution of 0.1 M aniline and 0.1 M H_2SO_4 (under nitrogen atmosphere) between -0.2 V and 0.85 V (vs. SCE) with a scan rate of 50 mV/s for 6 cycles to form a PANI/OMC/GCE. Finally, the PANI/OMC/GCE was scanned by cyclic voltammetry in a solution of 5 mM MES and 0.1 M H_2SO_4 between -0.2 V and 0.85 V (vs. SCE) at 50 mV/s for 4 cycles to form a PANI-MES/OMC/GCE. The modified electrode was then washed with ultrapure water and dried in air before use. The OMC/GCE and PANI/OMC/GCE were similarly prepared. The schematic diagram of the electrode preparation was illustrated in Scheme 1.

2.4 Analytical Procedure

DPASV was carried out for simultaneous determination of trace Cd^{2+} and Pb^{2+} in 0.1 M acetate buffer solution (pH 4.5) containing 1 μM Bi^{3+} . The DPASV method includes two processes: preconcentration and stripping. In the preconcentration process, the preconcentration potential of -1.2 V and preconcentration time of 150 s were applied to the working electrode under stirring conditions, so that the target metals and bismuth were deposited on the electrode surfaces. After the preconcentration, the stirring was stopped to reach an equilibration for 30 s. In the stripping process, the DPASV was recorded between -1.0 V and 0.2 V, and the voltammograms were recorded automatically. The electrode was cleaned at 0.3 V for 60 s under stripping conditions to remove the residual metals and bismuth film on the surface. Different concentrations of Cd^{2+} and Pb^{2+} ranged from 1 to 120 nM were measured in the experiment. The optimization of experimental parameters (e.g., PANI disposition, preconcentration potential, preconcentration time, and bismuth concentra-



Scheme 1. Schematic diagram of the preparation of the working electrode and analysis of Cd^{2+} and Pb^{2+} .

tion) was performed in acetate buffer solution with addition of 20 nM Cd^{2+} and 20 nM Pb^{2+} . A series of interference ions were adding to the acetate buffer solution to make interference study. All experiments were performed at room temperature.

3 Results and Discussion

3.1 Characterization of the Composite Materials on the Electrode

SEM images of OMC/GCE (A), PANI/OMC/GCE (B) and PANI-MES/OMC/GCE (C) are shown in Figure 1. Figure 1 A shows that OMC was made up of carbon nanorods with highly ordered structure, and the average length was about 1 μm . The GCE surface was evenly covered with OMC. Then PANI was electrochemically deposited on OMC by cyclic voltammetry method. The PANI with special space grid structure consist of nanorods and grows around the OMC are shown in Figure 1 B. Figure 1 C displays a typical morphology of PANI-MES/OMC/GCE, and MES completely covers the electrode surface.

3.2 Electrochemical Behavior

Electrochemical impedance spectroscopy (EIS) and DPASV were used to investigate the characteristics of different modified electrodes (bare GCE, OMC/GCE, PANI/OMC/GCE and PANI-MES/OMC/GCE).

EIS of $[\text{Fe}(\text{CN})_6]^{3-/4-}$ is used to provide information about the interface properties and impedance changes in the process of electrode modification [28]. The interface can be modeled by an equivalent circuit which includes the electron-transfer resistance (R_{ct}), the Warburg impedance (Z_{w}), the ohmic resistance of the electrolyte (R_s), and interfacial capacitance (C_{dl}) [27,29]. The Nyquist plot of impedance spectra includes two portions, a semicircle portion at higher frequencies corresponds to the electron-transfer resistance, and a linear portion at lower frequencies corresponds to the diffusion process [30]. As seen in Figures S1 and S2 (Supporting Information), the good agreement between the measured data and the fitting curve indicates that this equivalent circuit (Figure S3) is suitable and meaningful for this electrochemical system.

Figure 2 exhibits the Nyquist diagrams of the different modified electrodes, and the inset depicted the equivalent circuit. The bare GCE has a relative large R_{ct} value (412.4 Ω , Table S1, Supporting Information). After the

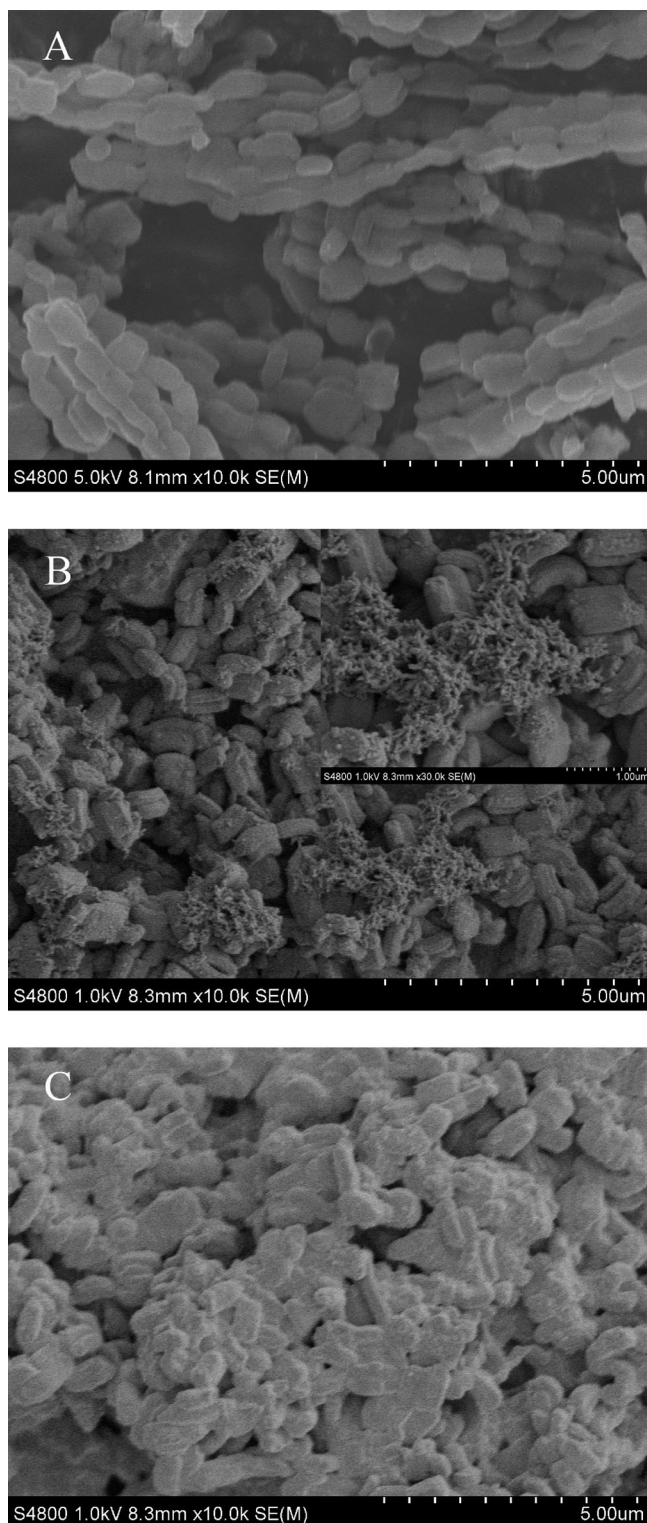


Fig. 1. SEM images: OMC/GCE (A), PANI/OMC/GCE (B), PANI-MES/OMC/GCE (C).

modification of OMC, the Nyquist plot presented an almost straight line which indicated a very small R_{ct} of OMC/GCE. Superior electrical conductivity of OMC that can accelerate the electron transfer on the electrode was proved here. The R_{ct} value had a very small increase after

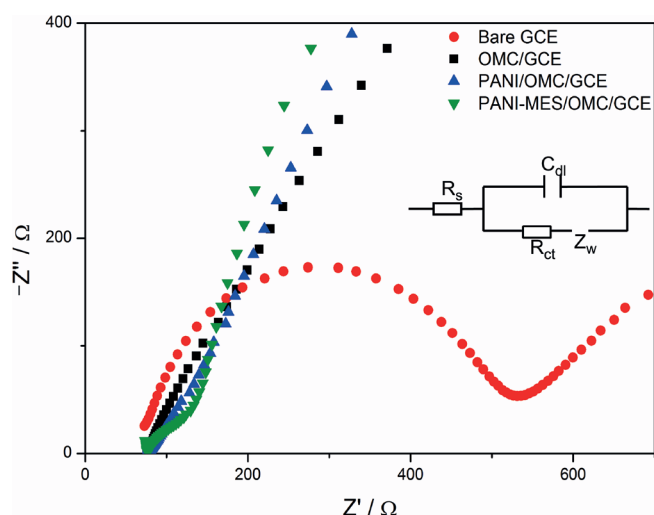


Fig. 2. Nyquist diagrams of bare GCE, OMC/GCE, PANI/OMC/GCE and PANI-MES/OMC/GCE using a 5.0 mM $[\text{Fe}(\text{CN})_6]^{3-/4-}$ solution containing 0.1 M KCl, with frequency range of 0.01–100 Hz, a bias potential of 0.2 V vs. SCE and an AC amplitude of 5 mV.

modification of PANI. Further deposition of MES slightly raised the R_{ct} . This increase indicated that the MES was successfully bound to PANI chains. Although the introduction of PANI film and MES did not further increase electrical conductivity of modified electrode, they provided large surface area and more binding sites with heavy metal ions, and these were the most important.

Figure 3 shows the DPASV response of different modified electrodes in 0.1 M acetate buffer solution (pH 4.5) containing 1 μM Bi^{3+} , 20 nM Cd^{2+} and Pb^{2+} . The stripping peak current of the modified electrodes increased in the order of Bi/GCE, Bi/OMC/GCE, Bi/PANI/OMC/GCE, and Bi/PANI-MES/OMC/GCE. Bi/GCE got the minimum response. The response of Bi/OMC/GCE was about two times larger than that of Bi/GCE, which is ascribed to the large surface area of OMC. The stripping peak current of Bi/PANI-MES/OMC/GCE was enhanced by 60% comparing with Bi/PANI/OMC/GCE, which would be interpreted as the addition of MES. On the Bi/PANI-MES/OMC/GCE surface, the sulfonic group of MES with negative charge could electrostatic adsorption of Cd^{2+} and Pb^{2+} ions (electrostatic factor), meanwhile, the sulfur atom could coordinate with Cd^{2+} and Pb^{2+} ions (coordination factor) [19]. The thiolated PANI exhibited better enrichment ability of Cd^{2+} and Pb^{2+} than PANI. The highest peak current observed from the Bi/PANI-MES/OMC/GCE indicated that the combination of OMC and PANI-MES achieved a good effect and was suitable for trace Cd^{2+} and Pb^{2+} determination.

3.3 Optimization of Experimental Parameters

All the optimal experiments were carried out by changing one parameter while keeping all other parameters con-

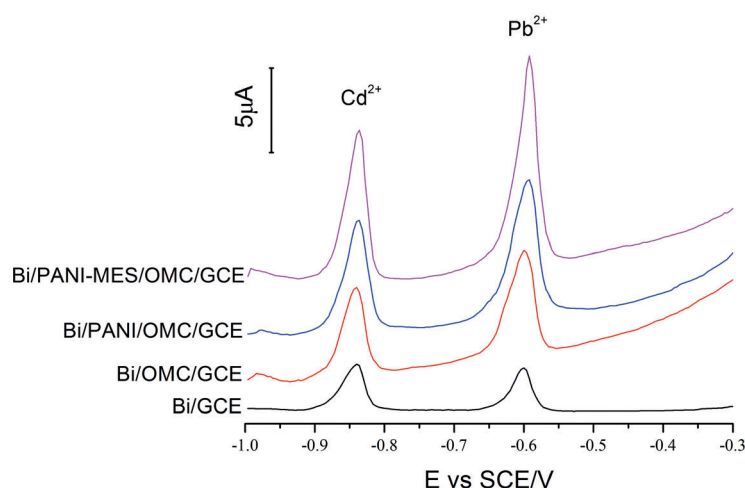


Fig. 3. Differential pulse anodic stripping voltammograms of 20 nM Cd²⁺ and Pb²⁺ in 0.1 M acetate buffer solution (pH 4.5) containing 1 μM Bi³⁺ using different modified electrodes. Preconcentration potential −1.2 V, preconcentration time 150 s, increment potential 0.004 V, amplitude 0.05 V, pulse width 0.2 s, sample width 0.0167 s, pulse period 0.5 s.

stant. The concentrations of Cd²⁺ and Pb²⁺ were kept at 20 nM.

3.3.1 Optimization of Supporting Electrolyte

A suitable supporting electrolyte is important for electrochemical determination. The supporting electrolyte can influence the electrochemical response of the analyte as well as the electrochemical activity of the working electrode [31]. PANI has a good electrical conductivity in acid solution, therefore, KCL(HCL), phosphate buffer solution and acetate buffer solution were selected (each 0.1 M) as the candidate electrolyte. The results showed that the highest peak current was obtained in 0.1 M acetate buffer solution (pH 4.5 as optimized). Therefore, acetate buffer solution (0.1 M, pH 4.5) was employed as supporting electrolyte.

3.3.2 Optimization of Preconcentration Potential and Preconcentration Time

Because the stripping potential of Cd²⁺ was found around −0.83 V and a more negative potential (< −1.3 V) would cause hydrolysis, the optimization of preconcentration potential was selected between −1.0 V to −1.3 V. In Fig. 4A, the stripping peak current increased gradually for both Cd²⁺ and Pb²⁺ when the potential shifted from −1.0 V to −1.2 V and reached a relative higher peak current at −1.2 V. As the potential became more negative, the stripping peak current decreased because the hydrogen evolution was beginning. The generated hydrogen bubble could damage the electrode surface and hinder the heavy metals enrichment [32]. Therefore, preconcentration potential of −1.2 V was employed for subsequent measurements.

In addition, preconcentration time was also optimized (Figure 4B). It was found that the stripping peak current

increased rapidly with preconcentration time from 50 s to 150 s. A longer preconcentration time could accumulate more heavy metals on electrode surface, led to the increase of stripping peak current. After 150 s, the effect of preconcentration time was insignificant, and the peak current almost remained constant. This phenomenon was ascribed to electrode surface saturation, attainment equilibrium [33,34], and probable exhaustion of solution-state target metals [11]. Therefore, 150 s was selected as the optimal preconcentration time and used in subsequent studies.

3.3.3 Optimization of Bismuth Concentration

Bismuth ion is easy to form binary-or multicomponent (low-temperature melting) ‘fusible’ alloys with various heavy metals, including cadmium and lead [35]. The thickness of bismuth film influences the formation of Bi alloys (with Cd²⁺, Pb²⁺) and enrichment of Cd²⁺ and Pb²⁺, and thus further influence the DPASV-analysis sensitivity. In this optimization experiment, the thickness of bismuth film can be controlled by its ion concentration in buffer solution. As Figure 4C shows, the stripping peak current of Cd²⁺ and Pb²⁺ linearly increased with Bi³⁺ concentration ranging from 250 nM to 1 μM. We could observe that the peak current increase of Pb²⁺ is smaller than Cd²⁺, that is because Pb²⁺ has more positive stripping voltage and can be determined at lower Bi³⁺ concentration [14]. Then, no obvious increase of peak current was found over 1 μM of Bi³⁺ concentration which was considered as the saturation of bismuth film. Meanwhile, the higher Bi³⁺ concentration would also cause competitive enrichment between Bi³⁺ and target metals on electrode surface. Synthesizing the above analysis, optimal bismuth concentration of 1 μM was selected.

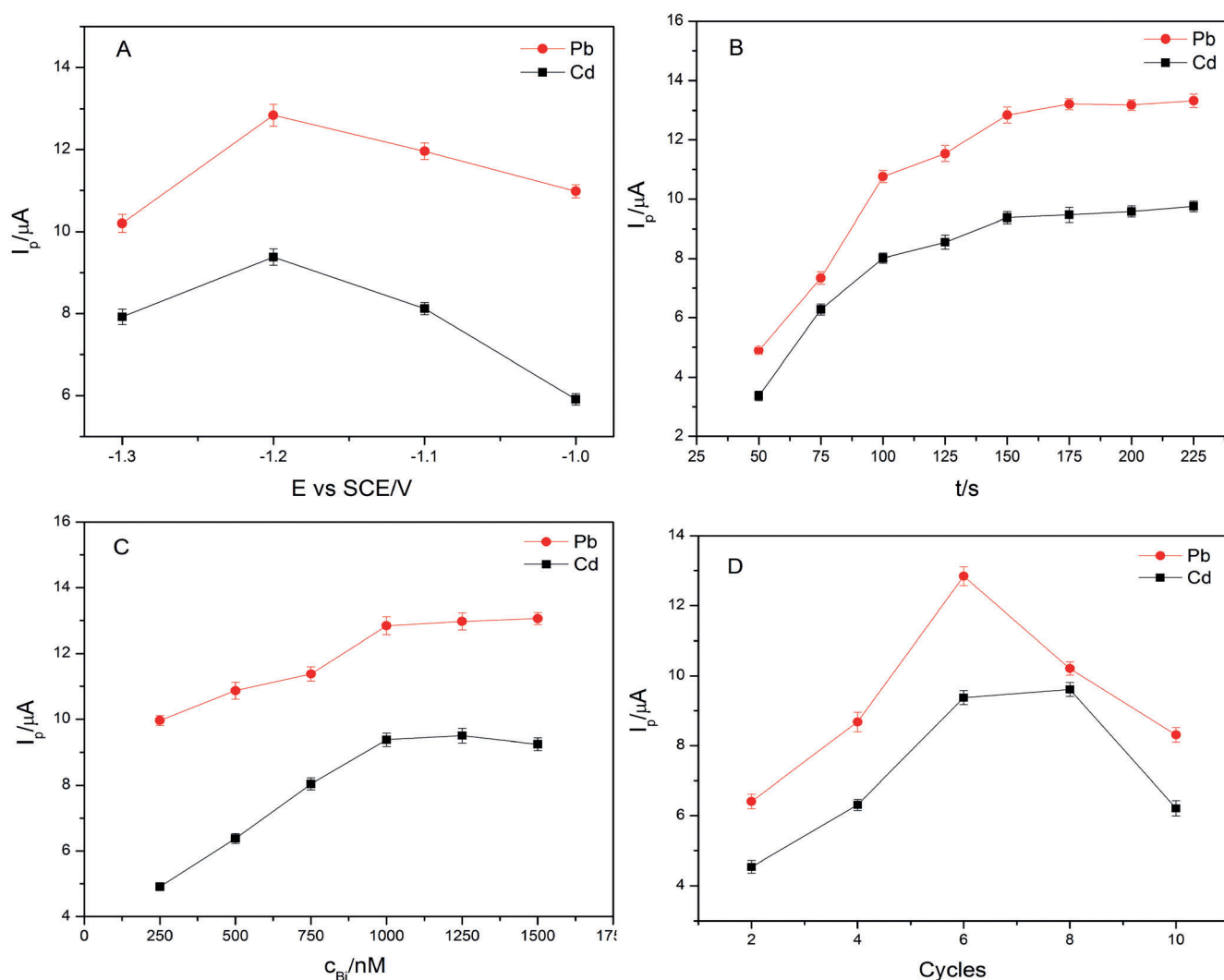


Fig. 4. Effects of (A) preconcentration potential, (B) preconcentration time, (C) Bi^{3+} concentration and (D) PANI deposition cycles on stripping peak current of 20 nM Cd^{2+} and Pb^{2+} . Other conditions are the same as Figure 3.

3.3.4 Optimization of PANI and MES Deposition

The thickness of PANI film is related to the aniline concentration and deposition time. In this study, cyclic voltammetry was used for electrochemical deposition of PANI film on electrode surface. The aniline concentration was certain, thus the thickness depended on the cycles of cyclic voltammetry. Therefore the thickness of PANI film would limit electrical conductivity and decrease the surface area, while, a thicker PANI film would also decrease the conductivity. An appropriate PANI film thickness was shown in Fig. 4D. The highest stripping peak current was obtained at 6 cycles for Pb^{2+} and 8 cycles for Cd^{2+} . We selected 6 cycles as the PANI deposition cycles and both Cd^{2+} and Pb^{2+} could achieve a relative higher current response. Optimization of MES deposition was also investigated (not shown) and 4 cycles of MES deposition could achieve the best response.

3.4 DPASV Analysis of Cd^{2+} and Pb^{2+}

Simultaneous determination of Cd^{2+} and Pb^{2+} with concentrations increase in the range of 1–120 nM was recorded to evaluate the electrochemical performance of Bi/PANI-MES/OMC/GCE under optimum conditions. The analysis procedure was described in Section 2.4. As shown in Figure 5, the stripping potential was -0.83 V for Cd^{2+} and -0.58 V for Pb^{2+} . The peak currents increased linearly with the increase concentration of both Cd^{2+} and Pb^{2+} with a slope of $0.4454 \mu\text{A nM}^{-1}$ and $0.5707 \mu\text{A nM}^{-1}$, respectively. The sensitivities (slope) is desirable. The linear fitting regression equations for Cd^{2+} and Pb^{2+} determination were obtained as $I_p (\mu\text{A}) = 0.7073 + 0.4454c$ (nM) and $I_p (\mu\text{A}) = 1.7746 + 0.5707c$ (nM), respectively. And the correlation coefficients were 0.9990 (Cd^{2+}) and 0.9988 (Pb^{2+}). Detection limits were estimated to be 0.26 nM (Cd^{2+}) and 0.16 nM (Pb^{2+}), according to the 3-sigma method (based on independent blank measure-

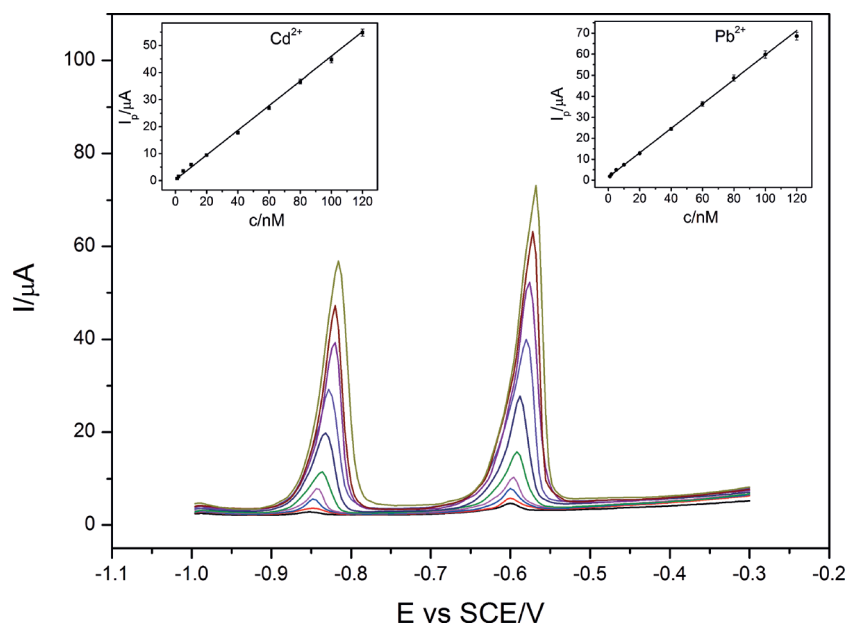


Fig. 5. Differential pulse anodic stripping voltammograms at different concentrations (1, 2, 5, 10, 20, 40, 60, 80, 100 and 120 nM) of Cd^{2+} and Pb^{2+} using Bi/PANI-MES/OMC/GCE under optimum conditions. The insets show the calibration plots. Other conditions are the same as Figure 3.

ments). Compared with the reported results by Chen et al. [20], the resulted $LODs$ of both Cd^{2+} and Pb^{2+} here have been improved. Table 1 showed the performance comparison of some modified carbon and CPs electrodes reported for the determination of Cd^{2+} and Pb^{2+} . The proposed electrode was the lowest one among them.

3.5 Repeatability, Reproducibility, and Interference

The repeatability of the proposed electrode was investigated by successive measurements ($N=5$) in the presence of 20 nM Cd^{2+} and Pb^{2+} under optimum conditions. After each measurement, the working electrode was transferred into the blank electrolyte, scanned at 0.3 V for 60 s to remove any adsorbed species. A satisfied repeatability was received with RSD of 2.8% for Cd^{2+} and 3.4% for Pb^{2+} . Reproducibility was studied by preparing

five proposed electrodes based on the above mentioned procedure and applied to the determination of 20 nM Cd^{2+} and Pb^{2+} . Under optimum conditions, the $RSDs$ of five independent electrodes were 3.1% for Cd^{2+} and 4.1% for Pb^{2+} , indicating that the fabrication procedure was reliable and the proposed electrode had good reproducibility. The electrode also had good long-term-storage stability after one week of storage. All the results showed the good performance of the proposed sensor.

The anti-interference ability of modified electrode is crucial for the electrode's practical application. In order to examine the anti-interference ability of the proposed sensor, various cations and anions were added to the acetate buffer solution containing 20 nM Cd^{2+} and Pb^{2+} for DPASV analysis under optimum conditions. The results showed that 100-fold concentration ratio of Ca^{2+} , Mg^{2+} , Cl^- , PO_4^{3-} , K^+ and SO_4^{2-} , 50-fold concentration ratio of Co^{2+} , CO_3^{2-} , Zn^{2+} , and 20-fold concentration ratio of

Table 1. Comparison of some carbon and CPs modified electrodes reported for the determination of Cd^{2+} and Pb^{2+} using anodic stripping voltammetry.

Electrode	Method	Limit of detection (LOD) (nM)		Reference
		Cd^{2+}	Pb^{2+}	
Bi/GCE	SWASV	–	5.31	[36]
Bi/PANI/GCE	SWASV	1.10	16.50	[21]
SWNTs-Nafion/GCE	DPASV	4.00	–	[37]
Nafion/OMC/GCE	DPASV	–	4.60	[38]
Bi/Nafion/2,2-bipyridyl/GCE	SWASV	1.10	0.37	[39]
Bi/Nafion/GCE	SWASV	0.89	0.48	[40]
Bi/Nafion/PANI-MES/GCE	SWASV	0.35	0.24	[20]
Bi/Nafion/OPPy-MES/GCE	SWASV	0.44	0.33	[11]
Bi/PANI-MES/OMC/GCE	DPASV	0.26	0.16	Present study

Table 2. Determination of Cd^{2+} and Pb^{2+} in real samples.

Samples	Original (nM)		Added (nM)		Proposed sensor nM		Recovery (%)		ICP-MS (nM)	
	Cd^{2+}	Pb^{2+}	Cd^{2+}	Pb^{2+}	Cd^{2+}	Pb^{2+}	Cd^{2+}	Pb^{2+}	Cd^{2+}	Pb^{2+}
Tap water	–	6.23	20.00	20.00	20.83	26.35	104.15	100.46	20.29	26.07
River water	19.46	25.78	20.00	20.00	39.29	44.17	99.57	96.48	38.08	46.11
Lake water	14.50	17.92	20.00	20.00	34.02	37.45	98.60	98.76	33.45	38.53

Fe^{3+} , Hg^{2+} and Ni^{2+} presented less than 5 % of peak current decrease. Copper has a relative large influence. 20-fold concentration ratio of Cu^{2+} presented 11 % peak current decrease. While 10-fold concentration ratio of Cu^{2+} resulted in less than 5 % peak current decrease. Therefore, the proposed sensor has a good anti-interference ability, and most of the common ions had little influence on the determination of Cd^{2+} and Pb^{2+} .

3.6 Application to Real Samples

In order to evaluate the application of the proposed sensor in real sample analysis, three different real samples (tap water, fresh river water from Xiangjiang and lake water from Taozi Lake) were collected, and the proposed sensor was employed for the determination of Cd^{2+} and Pb^{2+} . The real samples were filtered with a $0.45\ \mu\text{m}$ membrane (purchased from Millipore), adjusted to pH 4.5 using acetate buffer solution with $1\ \mu\text{M}$ Bi^{3+} added. The recovery was found to be from 96.48 % to 104.15 %, and measurement results obtained by proposed sensor were also in good agreement with ICP-MS method (Table 2). The comparative result showed that the proposed sensor has good accuracy and recovery, suggesting the great application potential in real samples.

4. Conclusions

A Bi/PANI-MES/OMC/GCE has been successfully developed and used for simultaneous voltammetric determination of trace Cd^{2+} and Pb^{2+} by DPASV method. The excellent properties of OMC (uniform pore structure, high specific surface area and fast electron transfer rate) and PANI-MES (high electrical conductivity, enhanced enrichment ability) contributed to the superior performance of the proposed electrode, such as high electrochemical sensitivity, lower detection limit and good capability of anti-interference. Applicability in real samples of proposed electrode was also verified. Novel materials based on thiolene chemistry would be an interesting research topic, and the combination of carbon materials and thiolated-CPs in electrode fabrication would give us an alternative route to develop new type of electrodes for heavy metals determination.

Acknowledgements

The study was financially supported by The Young Top-Notch Talent Support Program of China (2012), the Na-

tional Natural Science Foundation of China (51222805), the Program for New Century Excellent Talents in University from the Ministry of Education of China (NCET-11-0129), Interdisciplinary Research Project of Hunan University, Foundation for the Author of Excellent Doctoral Dissertation of Hunan Province, and Hunan Provincial Innovation Foundation for Postgraduate (CX2009B080).

References

- [1] I. A. Darwish, D. A. Blake, *Anal. Chem.* **2002**, 74, 52.
- [2] M. G. Tan, G. L. Zhang, X. L. Li, Y. X. Zhang, W. S. Yue, J. M. Chen, Y. S. Wang, A. G. Li, Y. Li, Y. M. Zhang, Z. C. Shan, *Anal. Chem.* **2006**, 78, 8044.
- [3] L. F. Dias, G. R. Miranda, T. D. Saint'Pierre, S. M. Maia, Vera L. A. Frescura, A. J. Curtius, *Spectrochim. Acta B* **2005**, 60, 117.
- [4] P. J. Zhang, G. Q. Xu, J. Lv, J. W. Cui, Z. X. Zheng, Y. C. Wu, *J. Electroanal. Chem.* **2012**, 685, 91.
- [5] V. K. Gupta, M. L. Yola, N. Atar, A. O. Solak, L. Uzun, Z. Üstündag, *Electrochim. Acta* **2013**, 105, 149.
- [6] M. Strouhal, R. Kizek, J. Vacek, L. Trnková, M. Němec, *Bioelectrochemistry* **2003**, 60, 29.
- [7] R. Güell, G. Aragay, C. Fontàs, E. Anticó, A. Merkoçi, *Anal. Chim. Acta* **2008**, 627, 219.
- [8] E. A. McGaw, G. M. Swain, *Anal. Chim. Acta* **2006**, 575, 180.
- [9] G. H. Hwang, W. K. Han, J. S. Park, S. G. Kang, *Sens. Actuators B, Chem.* **2008**, 135, 309.
- [10] D. Yang, L. Wang, Z. L. Chen, M. Megharaj, R. Naidu, *Electrochim. Acta* **2014**, 132, 223.
- [11] L. Chen, Z. Li, Y. Meng, P. Zhang, Z. H. Su, Y. Liu, Y. Huang, Y. P. Zhou, Q. J. Xie, S. Z. Yao, *Sens. Actuators B, Chem.* **2014**, 191, 94.
- [12] G. Aragay, J. Pons, A. Merkoçi, *Chem. Rev.* **2011**, 111, 3433.
- [13] E. A. Hutton, S. B. Hocevar, B. Ogorevc, M. R. Smyth, *Electrochem. Commun.* **2003**, 5, 765.
- [14] G. H. Hwang, W. K. Han, J. S. Park, S. G. Kang, *Talanta* **2008**, 76, 301.
- [15] M. Zhou, L. Shang, B. L. Li, L. J. Huang, S. J. Dong, *Biosens. Bioelectron.* **2008**, 24, 442.
- [16] Y. Y. Zhou, L. Tang, G. M. Zeng, Y. Zhang, Z. Li, Y. Y. Liu, J. Chen, G. D. Yang, L. Zhou, S. Zhang, *Anal. Methods* **2014**, 6, 2371.
- [17] J. C. Ndamaniha, L. P. Guo, *Bioelectrochemistry*, **2009**, 77, 60.
- [18] F. Li, J. X. Song, C. S. Shan, D. M. Gao, X. Y. Xu, L. Niu, *Biosens. Bioelectron.* **2010**, 25, 1408.
- [19] Z. Guo, S. Li, X. M. Liu, Y. P. Gao, W. W. Zhang, X. P. Ding, *Mater. Chem. Phys.* **2011**, 128, 238.
- [20] L. Chen, Z. H. Su, X. H. He, Y. Liu, C. Qin, Y. P. Zhou, Z. Li, L. H. Wang, Q. J. Xie, S. Z. Yao, *Electrochem. Commun.* **2012**, 15, 34.

- [21] Z. M. Wang, H. W. Guo, E. Liu, G. C. Yang, N. W. Khun, *Electroanalysis* **2010**, 22, 209.
- [22] M. D. Imisides, R. John, P. J. Riley, G. G. Wallace, *Electroanalysis* **1991**, 3, 879.
- [23] J. W. Chan, C. E. Hoyle, A. B. Lowe, *J. Am. Chem. Soc.* **2009**, 131, 5751.
- [24] R. M. Hensarling, V. A. Doughty, J. W. Chan, D. L. Patton, *J. Am. Chem. Soc.* **2009**, 131, 14673.
- [25] Y. Liu, Z. H. Su, Y. Zhang, L. Chen, T. A. Gu, S. Y. Huang, Y. Liu, L. G. Sun, Q. G. Xie, S. Z. Yao, *J. Electroanal. Chem.* **2013**, 709, 19.
- [26] S. Jun, S. H. Joo, R. Ryoo, M. Kruk, M. Jaroniec, Z. Liu, T. Ohsuna, O. Terasaki, *J. Am. Chem. Soc.* **2000**, 122, 10712.
- [27] L. Tang, Y. Y. Zhou, G. M. Zeng, Z. Li, Y. Y. Liu, Y. Zhang, G. Q. Chen, G. D. Yang, X. X. Lei, M. S. Wu, *Analyst* **2013**, 138, 3552.
- [28] G. M. Zeng, Z. Li, L. Tang, M. S. Wu, X. X. Lei, Y. Y. Liu, C. Liu, Y. Pang, Y. Zhang, *Electrochim. Acta* **2011**, 56, 4775.
- [29] L. Tang, G. M. Zeng, G. L. Shen, Y. P. Li, C. Liu, Z. Li, J. Luo, C. Z. Fan, C. P. Yang, *Biosens. Bioelectron.* **2009**, 24, 1474.
- [30] L. N. Zou, Y. F. Zhang, H. L. Qin, B. X. Ye, *Electroanalysis* **2009**, 21, 2563.
- [31] D. Sun, Z. M. Sun, *J. Appl. Electrochem.* **2008**, 38, 1223.
- [32] H. Bagheri, A. Afkhami, H. Khoshafar, M. Rezaei, A. Shirzadmehr, *Sens. Actuators B, Chem.* **2013**, 186, 451.
- [33] J. F. Ping, J. Wu, Y. B. Ying, M. H. Wang, G. Liu, M. Zhang, *J. Agric. Food. Chem.* **2011**, 59, 4418.
- [34] A. Afkhami, H. Bagheri, H. Khoshafar, M. S. Tehrani, M. Tabatabaee, A. Shirzadmehr, *Anal. Chim. Acta* **2012**, 746, 98.
- [35] J. Wang, *Electroanalysis* **2005**, 17, 1341.
- [36] J. Wang, J. M. Lu, S. B. Hocevar, P. A. M. Farias, *Anal. Chim. Acta* **2000**, 72, 3218.
- [37] D. Sun, X. F. Xie, Y. P. Cai, H. J. Zhang, K. B. Wu, *Anal. Chim. Acta* **2007**, 581, 27.
- [38] L. D. Zhu, C. Y. Tian, R. L. Yang, J. L. Zhai, *Electroanalysis* **2008**, 20, 527.
- [39] F. Torma, M. Kádár, K. Tóth, E. Tatár, *Anal. Chim. Acta* **2008**, 619, 173.
- [40] G. Kefala, A. Economou, A. Voulgaropoulos, *Analyst* **2004**, 129, 1082.

Received: July 13, 2014

Accepted: August 24, 2014

Published online: September 24, 2014